Studies of parallel and tilted vortices in type-II superconductors by microwave absorption

P. Monceau
Centre National de la Recherche Scientifique-Centre Recherche sur les Très Basses Tempêratures B.P. 166, F 38042 Grenoble, France

D. Saint-James
Laboratoire de Physique des Solides de l'ENS, Tour 23, Université Paris VII 9, quai Saint-Bernard, F 75005 Paris, France

G. Waysand
Laboratoire de Physique des Solides, Bâtiment 510, Université Paris-Sud, Centre d'Orsay,F91405, France
(Received 17 June 1974)

A general study is made of the observation of size effects in type-II superconducting films by microwave absorption. A new class of size effects is presented that we attribute to the interference of tilted vortices (generated by a tilted magnetic field on the sample) with the surface sheath. A putative geometrical model is presented, which is in good agreement with experimental data. An extension of this model is made to multilayered superconductive compounds (dichalcogenides).

I. INTRODUCTION

When the thickness d of type-II superconducting film is just equal to its critical value (that is to say to 1.8 times the coherence length ξ) the electromagnetic properties just under the critical parallel magnetic field, as it is known, exhibit a discontinuity. This size effect has been observed by tunnel effect.[1] The purpose of this paper is to show that with microwave absorption, not only this size effect, but many others can be observed.

In Sec. II, we begin by reporting microwave experiments on that effect which is due to the penetration of a first row of vortices in the film. The same behavior occurs when the film can accommodate two, three, etc., rows of vortices and this also can be detected by microwave absorption. From the discussion of these experiments, the conditions of observation of size effects of vortex lattice by microwave absorption are defined.

In Sec. III, we extend this technique to the study of type-II superconductivity in tilted magnetic field on the surface. The theoretical situation of the subject is recalled. Then results are presented on the angular dependence of microwave absorption of bulk samples ($d \gg \xi$). This dependence exhibits many extrema. We interpret them in the frame of a very simple but putative model as a new type of size effects, namely, interference of tilted vortices with the surface sheath. The reasons why this model is only putative are discussed as well as the reproducibility of the measurements. In Sec. IV, we give other arguments in favor of our model of tilted vortices by applying it to the case of intercalated dichalcogenide superconducting compounds.

The experimental devices and the preparation of the samples are deferred to the appendix for convenience of presentation of the results.

II. SIZE EFFECTS IN PARALLEL FIELD

A. First entry in a thin film in the Ginzburg-Landau regime

The penetration of a parallel magnetic field around its critical thickness has already been studied by Guyon, Meunier, and Thompson[1] by tunnel-effect measurements done in the frame of the Ginzburg-Landau (GL) theory. A discontinuity in $dI(V)/dV$ taken at a subcritical value of the magnetic field is observed at the critical thickness of the film $d = 1.8\xi$. By varying the temperature, it is possible for a sample of chosen thickness to go through the adequate value of $\xi(T)$. This defines a temperature of first entry of the magnetic field in the film, T_{FE}. Thompson[2] has extended this result to the case of microwave absorption. The microwave conductivity of the sample, $\sigma = \sigma_1 - i\sigma_2$, is expressed by

$$\sigma_1 = L\left(\frac{\epsilon_0^2}{\omega^2+\epsilon_0^2} + 3\rho\,\frac{\psi''(\frac{1}{2}+\rho)}{\psi'(\frac{1}{2}+\rho)}\right), \tag{1}$$

$$\sigma_2 = -L\,\frac{2\epsilon_0}{\omega}\left(1+\frac{1}{2}\,\frac{\omega^2}{\omega^2+\epsilon_0^2}\right). \tag{2}$$

ψ' and ψ'' are the usual first and second derivatives of the digamma function and $\epsilon_0 = 2DeH_{c2}$ ($D = \frac{1}{3}V_F l$ is the diffusion coefficient for the electrons).

The common amplitude coefficient of σ_1 and σ_2 is expressed by

$$L = \frac{4D\sigma}{\epsilon_0}\,\frac{\langle|\Delta^2|\rangle}{|\Delta \pm \frac{1}{2}d|^2}\,J_1\,\frac{1.20\kappa_2^2}{\kappa_2^2 - J_2}\,(H_{c\parallel} - H). \tag{3}$$

J_1 and J_2 are two functions numerically calculated, and J_1 exhibits a discontinuity at the critical thick-

ness. In fact, J_1 and J_2 are the same functions for the tunnel effect as well as for surface impedance. The discontinuity in J_1 represents the passage from a nodeless variation of $\Delta(r)$ to a one-node variation. This discontinuity has been effectively observed by microwave absorption.[3] Figure 1(a) shows the results of an experiment on a *Pb*In (20 wt%) thin film of 2100 Å at 2.45 GHz. The reduced slope $(H_{c\parallel}/R_N)(\partial R_d/\partial H)$ taken in the subcritical region is plotted as a function of the reduced temperature, where R_d is the resistance of the superconducting film at H, T and R_N is the resistance of the film in the normal state. The predicted discontinuity is observed. It is of the same order of magnitude as the discontinuity of J_1 represented in the insert of Fig. 1.

The observation of the correct discontinuity requires the following conditions:

(i) Since we are in the subcritical region, the microwave absorption is controlled by the normal skin depth δ. This length ought to be much larger than the coherence length. Figure 2 represents the results of a quite systematic study of *In*Bi films in the X band. With these alloys and frequencies, not only a jump but also a change of sign occurs at T_{FE} as it was reported previously.[4] This anomalous behavior of *In*Bi films in the X band is largely due to the fact that in that case d and δ are of the same order of magnitude. As a result, the plane-wave approximation is no longer valid, contrary to what is assumed in Thompson's calculations.

(ii) If the condition $d \ll \delta$ is fulfilled, the discontinuity can be observed by microwave absorption only for $\kappa \gg 1$ superconductors. We never saw the discontinuity at T_{FE} for *Pb*In films (2.3 wt%): for this In concentration, $\kappa \sim 1$. Near $H_{c\parallel}$ the transition curves are rounded, consequently we have not enough precision to determine the slope.

(iii) Because of the condition $d \ll \delta$, the substrate and the wall of the resonator, on which the film is glued, controlled the absorption. This probably explained why, in contrast with the case of bulk samples, the transition curves $R(H)$ at a given temperature are linear only in the first few % of H starting from $H_{c\parallel}$. It is in this region that the slope has to be taken if a comparison is to be made with GL theory. For a slope taken on the steepest part of the transition curve, the discontinuity in $(H/R_N)(\partial R/\partial H)$ is no longer observed.

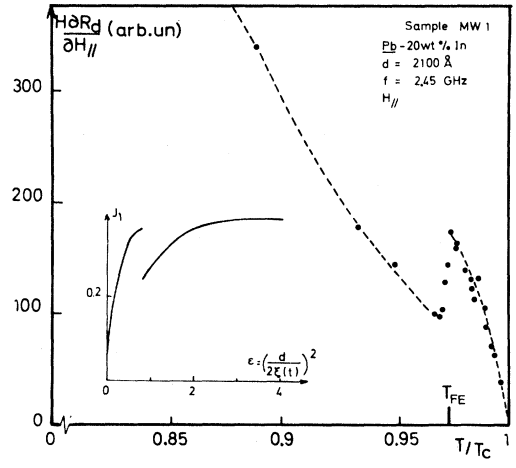

FIG. 1. Variation of the reduced slope $(H_{c\parallel}/R_N)(R_d/H)$ with the reduced temperature T/T_c. The discontinuity of $\frac{1}{3}$ observed at T_{FE} corresponds to the first penetration of the magnetic field in the sample. By measuring $H_{c\perp}$ and $H_{c\parallel}$, we have verified that $H_{c\parallel}/H_{c\perp} = 2$ and that $[d/2\xi(T)]^2 = 0.81$ (by applying $H_{c\perp} = \phi_0/2\pi\xi^2$). For that value of $[d/2\xi(T)]^2$ the insert shows that the function J_1, representative of the screening effect of the supercurrents, exhibits the same discontinuity.

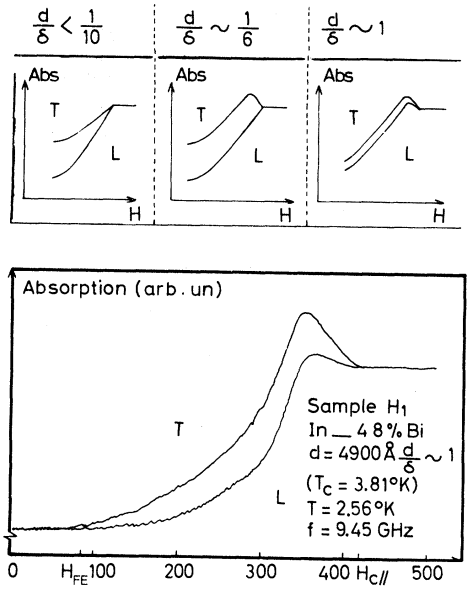

FIG. 2. Three upper graphs represent the variation of the absorption of an *In*Bi sample of critical thickness $(d = 1.8\xi)$ but for various ratio of d/δ (δ is the normal skin depth). The sign T refers to a magnetic field H parallel to the surface of the sample but in transverse orientation ($\vec{E}_\omega \perp \vec{H}$; $\vec{E}_\omega$ is the microwave electric field). The sign L refers to a magnetic field parallel to the surface in longitudinal orientation. A typical recording of the $d/\delta \sim 1$ situation is shown under the three graphs. It should be noted that even for $d/\delta \sim \frac{1}{6}$ the absorption exhibits an anomalous behavior in the transverse orientation. Thus, for the study of size effect, the condition $d/\delta \ll 1$ has to be carefully fulfilled.

B. Generalization to size effects in parallel magnetic field far from $H_{c\parallel}$

Starting from the critical thickness, one can, by decreasing the temperature, go to a situation where the film can accommodate not only one but also two, three, etc., rows of vortices. This was observed by tunnel effect by Sutton[5] in the following way: at low temperatures *Pb*In (20-wt%) films exhibit in the dI/dV curve versus H a series of dips corresponding to the penetration of a row of fluxoids. The same thing happens in the microwave impedance curve as a function of H, of equivalent samples as shown in Fig. 3. In this figure, the effect of penetration of one, two, and three rows of vortices can be seen. As for the tunnel effect, the detection of these size effects by microwave absorption is only possible for high-κ materials; we saw nothing but the regular plateau in the surface-impedance curve of *Pb*In 5-wt% films. Therefore, we can deduce from Secs. II A and II B that the observation of size effects by microwave absorption requires high-κ materials, whether or not we are in the GL regime. This is why we always use *Pb*In 10- or 20-wt% alloys for the study of size effects. We can turn now our attention to a new type of size effects: those of tilted vortices.

III. TILTED VORTICES

A. Review of the theoretical situation of type-II superconductivity in tilted fields

1. Angular dependence of the critical field

A bulk type-II superconductor in high field exhibits two remarkable regimes: (a) in perpendicular field, the critical field is H_{c2} and, for every field $H<H_{c2}$, the most energetically favorable structure against the flux penetration is, as it was shown by Abrikosov,[6] a vortex lattice; (b) in parallel field; in that case as it was shown by Saint-James and de Gennes, the critical field is $H_{c3}=1.69H_{c2}$. Only a surface sheath, the width of which is of the order of the coherence length, is superconducting. We have "surface superconductivity."

Thus, it is evident that superconductive properties are strongly dependent of the angle θ between the field and the surface of the sample. This is true for the critical magnetic field itself. This problem was first studied by Tinkham[7] who proposed a semiempirical formula to describe the angular dependence of the critical field $H_c(\theta)$:

$$\left(\frac{H_c(\theta)}{H_{c3}}\right)^2 \cos\theta + \frac{H_c(\theta)}{H_{c2}} \sin\theta = 1 . \tag{4}$$

This was obtained by assuming that the parallel and the perpendicular component of the critical field can be treated independently of each other. In fact, this is valid only for very thin films ($d/\xi \ll 1$). However, Saint-James[8] solved the Ginzburg-Landau equations by a perturbation method.

In the linear approximation, this equation can be written

$$D\left(i\frac{\partial}{\partial y}+\frac{2eH}{c}(x\sin\theta - z\cos\theta)\right)^2 \Delta - D\left(\frac{\partial^2}{\partial x^2}+\frac{\partial^2}{\partial z^2}\right)\Delta = \epsilon\Delta , \tag{5}$$

where the z axis is perpendicular to the surface and D the diffusion coefficient.

The condition to impose on Δ is

$$\frac{\partial\Delta}{\partial z} = 0 \quad \text{at } z = 0 . \tag{6}$$

Saint-James's calculation seeks for solution of the form

$$\Delta(\vec{r}) = e^{ik_0 y}\phi_0(x,z) \tag{7}$$

and considers two parts in the GL equation; one is a "nonperturbed" equation

$$-\frac{\partial^2\phi_0}{\partial x^2}-\frac{\partial^2\phi_0}{\partial z^2}+\left(k_0-\frac{2eH}{c}z\cos\theta\right)^2\phi_0 + \frac{4e^2H^2}{c^2}x^2\sin^2\theta\phi_0 = \frac{\epsilon}{D}\phi_0 , \tag{8}$$

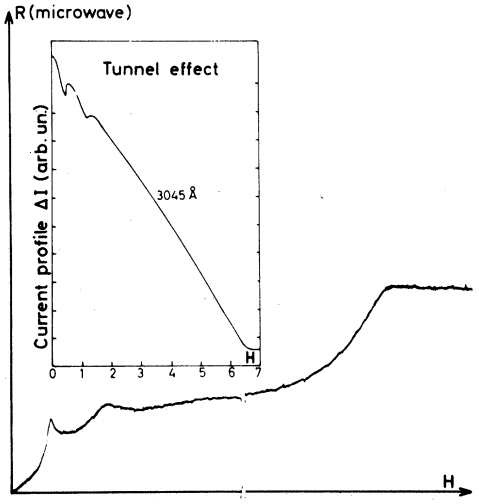

FIG. 3. Surface impedance at 2.45 GHz and $t=0.447$ of a *Pb* In (10-wt%) films of 3150 Å as a function of the parallel magnetic field, each change of slope corresponds to the penetration of a row of vortices. The insert represents the same effect detected by tunnel effect by Sutton for a *Pb* In (20-wt%) of 3045 Å at 4.2 °K.

and the second part is the cross term in x and z,

$$V = \frac{4eH}{c}\left(k_0 - \frac{2eH}{c} z\cos\theta\right) x\cos\theta , \tag{9}$$

which is treated as a perturbation.

The series of perturbation is then completely calculable in the limit $\theta \to 0$. Saint-James was able to express $[1/H_c(\theta)][\partial H_c(\theta)/\partial\theta]_{\theta=0}$ as a function of the reduced thickness d/ξ. For $d/\xi \to \infty$ this logarithmic derivative tends toward -1.35 (the same value was first found by Tinkham). The variation of $(1/H)(\partial H/\partial\theta)$ exhibits a rupture for $d \sim 1.8\xi$ (we recover here the situation of Sec. II of this paper). Finally, the calculation confirms the validity of the Tinkham's expression for $d/\xi \ll 1$.

However, this method cannot be extended to large angles. Yamafugi, Kasayanagi, and Irie chose to treat the same problem by a variational method.[9] They wrote the solution of the GL equation under the form

$$\Delta(x, y, z) = G(x)F(z)e^{ik_0 y} . \tag{10}$$

Again is present the Tinkham idea of factorization of the perpendicular direction (z) and the parallel direction (x). $G(x)$ is taken as a Gaussian and F is then calculated; a Weber function is found.

Finally, Yamafugi *et al.* proposed the following formula for $H_c(\theta)$:

$$\left(\frac{H_c(\theta)}{H_{c3}}\cos\theta\right)^2 [1 + \tan\theta(1 - \sin\theta)] + \frac{H_c(\theta)}{H_{c2}}\sin\theta = 1 . \tag{11}$$

All those results are compared in Fig. 4.

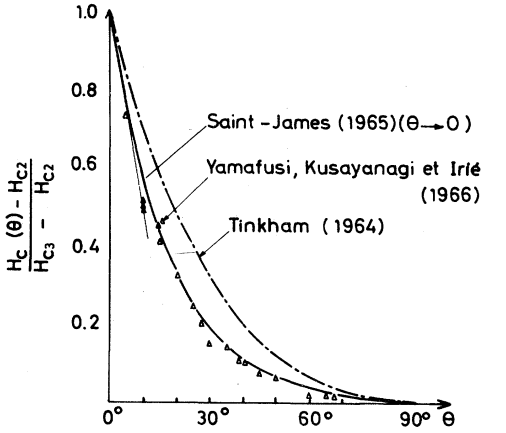

FIG. 4. Angular variation of the critical field of a type-II superconductor calculated for a thin film by Tinkham for a bulk sample by Saint-James (perturbation method) and Yamafugi *et al.* (variational method). The dots are experimental points of a bulk sample.

2. *Tilted vortices: generalization*

These different methods admit a periodic variation of the order parameter along the surface. In other terms, a vortex structure is assumed, the tilted vortex structure, different from the one created by the interference of the two surface sheath in parallel field as soon as $d > 1.8\xi$ (Sec. II B). Naturally, this second structure is expected to still exist if $\theta \sim 0$ but, as a first step, we can neglect it as long as $d/\xi \gg 1$.

In that case, Kulik[10] has examined the vortex structure in one surface sheath. The existence of such a structure can be understood if one looks to the variation of superconductivity in a bulk sample when one rotates the magnetic field from $\frac{1}{2}\pi$ to 0.

For $\theta = \frac{1}{2}\pi$, the critical field is H_{c2}, superconductivity spreads all over the thickness of the sample (the notion of surface sheath is meaningless in this orientation). We have the well-known Abrikosov structure of vortices. For $\theta \sim \frac{1}{2}\pi$, all the sample is still in the superconducting state but then we have yet tilted vortices (parallel to the field). If θ is decreased, the critical field increases and surface superconductivity is more and more present.

Under a given angle, the two surfaces sheath are separated one from the other. One expects to have two completely distinct surfaces sheath, each of them with its own vortex array. The tilted vortices or Kulik's vortices look like the fingers of a glove (Fig. 5). What is exactly this vortex structure? To answer this question, it is necessary to take into account, in Eq. (5), the nonlinear terms, to evaluate the force energy and finally to show that a periodic structure minimizes it. Kulik, in his paper, does not go that far. He simply shows that the linearized equation near $H_c(\theta)$ has periodic solutions. On other terms, Kulik searches the periodic solution of (5). However, the problem is still complex thanks to the presence of the cross term V [Eq. (9)]. Kulik writes the solution under the form of Eq. (7) but points out that

$$\Delta(\boldsymbol{r}) = \exp[i(k_0 + k')y]_x \phi_0[x + (k'\rho_0/2\sin\theta), z] \tag{12}$$

[where $\rho_0 = (\hbar c/eH)^{1/2}$] is also a solution.

The same remark was made by Abrikosov[6] when he studied the notion of vortex array near H_{c2}. From this remark, Kulik concludes to the possible existence of a vortex structure in each tegument as soon as the magnetic field is tilted on the surface.

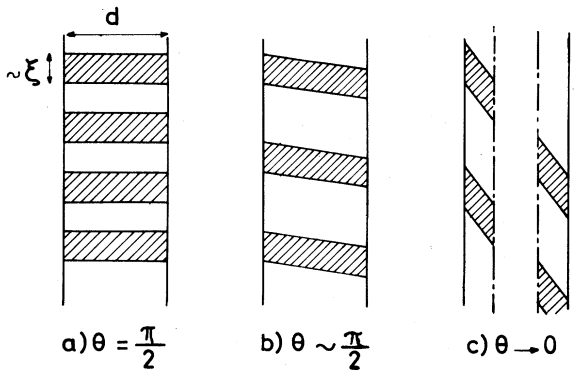

FIG. 5. Schematic representation of vortices in a bulk sample ($d >> \xi$). The darkened zones represent the vortex core. This is an oversimplification because near the critical field, the notion of vortex cores is meaningless, the distance between vortices being of the order of ξ. However, with this convention, case a ($\theta = \frac{1}{2}\pi$) is the well known H_{c2} situation; the vortex structure spreads all over the sample. This is still true in case b when the magnetic field is near the perpendicular direction. But in case c, under a given angle, the surfaces sheath are distinct and each of them has its own vortex structure.

In order to simplify the problem, Kulik considers a semi-infinite sample. This approximation is valid if θ is not too near from $\frac{1}{2}\pi$.

By analogy with the Abrikosov treatment, Kulik writes

$$\Delta(r) = \sum_{n=-\infty}^{+\infty} C_n \exp\left[i\left(k_0 + \frac{2\pi n}{\alpha}\right)y\right] \phi(x + n\beta, z). \quad (13)$$

A periodic structure is assumed along the surface with α and β as lattice parameters. Like in Abrikosov,[6] the value of different coefficients C_n determines the structure (i.e., for $\alpha = \beta$ and all the C_n equal the array is square, etc.).

For ϕ, Kulik takes the variational form

$$\phi(x, z) = \exp\left(-\frac{x^2}{2x_0^2}\right)\exp\left(-\frac{z^2}{2z_0^2}\right), \quad (14)$$

where

$$z_0 = \rho_0\left(\frac{\gamma}{2\cos\theta}\right)^{1/2}, \quad x_0 = \frac{\rho_0}{(2\sin\theta)^{1/2}} \quad (15)$$

are deduced by a variational method from Eq. (5).

However, in contrast with Abrikosov, *Kulik does not take in account,* as we said before, the *nonlinear term,* therefore he is not able to calculate and minimize the free energy, and *this does not allow him to determine the geometrical structure of the vortex lattice.* In fact, Kulik takes arbitrarily a square lattice *on the surface*; he writes $\alpha = \beta$.

To determine α and β, one needs the equation expressing the flux quantification: across one cell of the lattice, the magnetic flux is equal to one flux quantum $\phi_0 = \pi\hbar c/e$.

For a square lattice, this is expressed by

$$\alpha^2 \sin\theta = \phi_0/H(\theta), \quad (16)$$

$$\alpha = [1/(\sin\theta)^{1/2}]\phi_0/H(\theta), \quad (17)$$

$\alpha \to \infty$ when $\theta \to 0$. This expresses the disparition of the vortex structure in a parallel magnetic field.

From the work of Kulik, we will use two results for our model of tilted vortices: (i) the variation of z_0 with θ which is a consequence of the expression taken for the order parameter [Eq. (7)]; (ii) the condition of quantification that we write in a more general form

$$\mu ab \sin\theta = \phi_0/H(\theta) = \pi\rho_0^2, \quad (18)$$

where $\mu = \sin\phi$, ϕ is the angle between the two elementary vectors of the lattice. This equation can be written as soon as the field is no longer parallel to the surface. It expresses the quantification of the perpendicular component $H\sin\theta$ of the magnetic field. One can see the tilted magnetic field situation as the superposition of a surface sheath superconductivity resulting from the parallel component $H\cos\theta$ interacting with a vortex structure determined by the perpendicular component $H\sin\theta$. However, this interaction cannot be assimilated to a simple algebraical or vectorial addition.

Another important remark about the condition of flux quantification expressed by Eq. (18) is that it does not imply *a priori* that a and b are both varying with θ. It is only requested that their product fulfils (18). When $\theta \to 0$, a or b, or a and b together $\to \infty$.

3. *Microwave impedance and tilted vortices*

Microwave absorption of a bulk sample is very sensitive to tilted vortices. This fact was first observed by Monceau[11]; he was trying to adjust the field parallel to the sample and he noted that the best criterion for that was to maintain the field constant, slightly under its critical value and to look for a minimum resistance rather than for the higher critical field. Figure 6 represents the angular dependence of the microwave resistance R_ω for a bulk sample *Pb*In (10 wt%) at 4.2 °K and 2.45 GHz for various values of the applied field. A sharp variation of R_ω near the parallel orientation can be noted in the subcritical region (H slightly under 1.69 H_{c2}). To understand what occurs, let us assume that in the parallel orientation the electric component E_ω of the microwave field is parallel to the magnetic field. In other

terms, we are in the parallel longitudinal orientation ($\vec{E}_\omega \| \vec{H}_\parallel$) (see Fig. 7). As soon as the field is tilted, a vector $\vec{E}_\omega \times \vec{H}$ appears which puts the tilted vortices in a collective oscillation.[12] This creates a supplementary absorption. The best evidence of this supplementary absorption was put in evidence by the so-called anisotropy of the surface impedance[13]; in the parallel orientation ($H_\parallel \lesssim H_{c3}$) the microwave absorption is higher in the parallel transverse orientation ($\vec{H}_\parallel \perp \vec{E}_\omega$) than in the parallel longitudinal one ($\vec{H}_\parallel \| \vec{E}_\omega$). This surface impedance anisotropy is the continuation in the microwave range of the flux-flow phenomenon in dc measurements. Both take place only when the order parameter has a spatial variation (vortex lattice or surface sheath). In that sense, the sharp variation of R_ω around the parallel orientation is an indirect proof of the existence of tilted vortices. However, to evaluate this variation, a theoretical approach is needed. It was provided by Maki in two different ways. The first[14] is in the spirit of the Yamafugi and co-workers' calculation of $H_c(\theta)$. The second[15] follows the work of Caroli and Maki on dynamic fluctuations of the order parameter.[12] As we will see hereafter, in both methods Maki does not take into account the geometrical structure of the lattice of tilted vortices.

Both methods lead to similar results. There is only a difference in the transverse orientation. Hereafter, we give the results of the second calculation which is more precise according to Maki.

There are different cases because we have to distinguish between the transverse and the longitudinal orientation (Fig. 7). The surface impedance introduces a second distinction. Effectively, we have not only the three usual characteristic lengths of a surface-impedance problem in superconductivity $\xi(T)$, d, δ (the normal skin depth) but also $e_t(\theta)$, the thickness of the tegument in the orientation θ. As we have yet noted, e_t varies from a length equivalent to $\xi(T)$ in the parallel orientation to $e_t(\frac{1}{2}\pi) \sim \infty$ in the perpendicular orientation. Thus, even if we are in a situation of extremely local electrodynamics [$\xi(T) \ll \delta$] by a simple rotation of the field, one can go from situations where the surface sheath is much smaller than the normal skin depth to opposite situations: $\delta \ll e_t(\theta)$. In our experiments, this situation is generally not realized because we very often work on "pseudobulk" samples: $\xi(T) \ll d \ll \delta$ (we defined the bulk samples by $d \gg \delta$). However, the electromagnetic absorption varies with e_t/δ. An approximate value of e_t can be obtained if, like Kulik, we assume a Gaussian variation of the order parameter

$$\Delta(z) = C \exp\left(-\frac{z^2}{2z_0^2}\right),$$

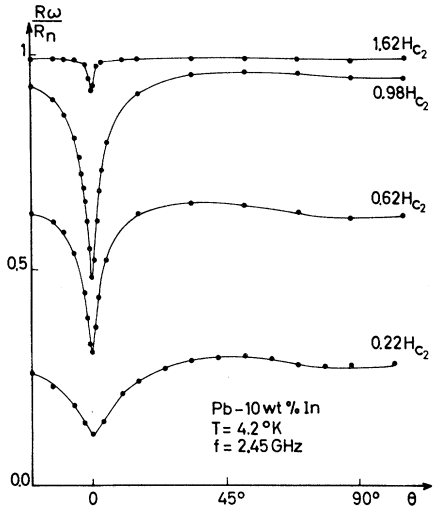

FIG. 6. Angular dependence of the microwave resistance R_ω of *Pb* In (10 wt%) at 4.2 °K for various applied fields. Around the parallel orientation ($\theta = 0°$), a sharp variation is noticed due to supplementary absorption created by dynamic fluctuations of tilted vortices. This experiment was done in transverse orientation $e_\omega \perp H$ when $\theta = 0$.

$$e_t = \int_0^\infty dz \exp\left(-\frac{z^2}{2z_0^2}\right) = \left(\frac{\pi}{2}\right)^{1/2} z_0$$
$$= \left(\frac{\delta \rho_0^2 \gamma}{4\cos\theta}\right)^{1/2} = \frac{1.18\,\xi(T)}{(\cos\theta)^{1/2}}. \quad (19)$$

In each orientation, the Maki results are, if we denote the microwave impedance of a bulk sample,

$$Z_\infty = R_\infty + iX_\infty, \quad (20)$$

longitudinal case and $e_t(\theta) \ll \delta$,

$$R_{S\infty} = R_{N\infty}\left(1 - \alpha(H,\theta)\frac{H_{c3}(\theta) - H}{H_{c3}(\theta)}\frac{\tilde{\omega}^2}{1+\tilde{\omega}^2}\right), \quad (21)$$

$$X_{S\infty} = R_{N\infty}\left(1 - \alpha(H,\theta)\frac{H_{c3}(\theta) - H}{H_{c3}}\frac{\tilde{\omega}^2}{1+\tilde{\omega}^2}\right), \quad (22)$$

with

$$\alpha(H,\theta) = \frac{\delta}{\xi(t)^2}\left(\frac{2\pi}{1.18eH\cos\theta}\right)^{1/2} \times \frac{1}{1.16[2\kappa_2^2(t) - 0.334\cos\theta - \sin\theta]}, \quad (23)$$

$$\tilde{\omega} = \omega/4eDH\sin\theta \quad \text{and} \quad t = T/T_c. \quad (24)$$

B. Experimental discussion of Maki's calculation on microwave angular dependence

Experimentally, in the microwave range, it is easier to look for the variation of the absorption of a cavity than for its frequency shift. If in this cavity one has a bulk sample of impedance

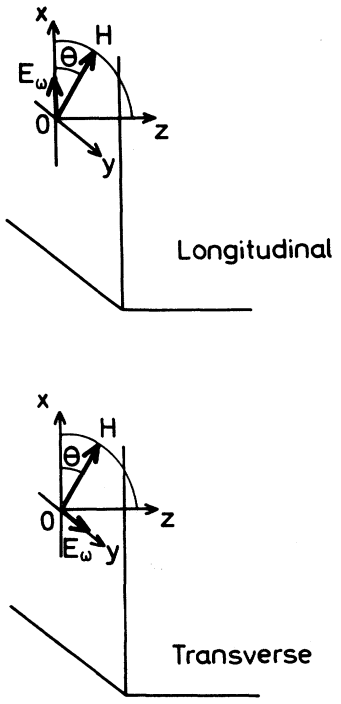

FIG. 7. Orientation of the magnetic field H and the microwave electric field e_ω in the tilted longitudinal and the tilted transversal orientation.

$$Z_\infty = R_\infty + iX_\infty ,$$

the absorption is proportional to R_∞. From Eqs. (21)–(24), we can deduce that for Maki there is a characteristic angle θ_c that we can define as

$$\theta_c = \omega/4eDH \tag{25}$$

for

$$\theta \ll \theta_c, \quad R_{S\infty} \gg X_{S\infty}, \tag{26}$$

$$\theta = \theta_c, \quad R_{S\infty} = X_{S\infty}, \tag{27}$$

$$\theta \gg \theta_c, \quad R_{S\infty} \ll X_{S\infty}. \tag{28}$$

Qualitatively, this is in good agreement with the initial work of Monceau[1] who has noted a very sharp decrease of R_∞ with θ. In his experiment θ_c can be estimated to be of the order of 0.15°. This value is too small to be quantitatively checked. Even in the X band θ_c hardly reaches 1° for PbIn alloys. On the other hand, as R_∞ decreases very sharply, one cannot hope that it will be very easy to measure precisely R_∞. Practically, there is no easy experimental verification of Maki's calculation if one does not turn to "pseudobulk" thin films, where $\xi \ll d \ll \delta$. These samples are thick from the point of view of the static properties of superconductivity but thin for the microwave absorption.

It is shown in Appendix B that the impedance

$$Z_d = R_d + iX_d \tag{29}$$

of a pseudobulk sample can be expressed, in the high-field region [H slightly under the angular critical field $H_c(\theta)$] in terms of R_∞ and X_∞.

For the absorption, one finds

$$R_d = (1/2\sqrt{2})(d/\delta)(R_\infty + X_\infty). \tag{30}$$

In the domain $\theta \gg \theta_c$, this implies

$$\frac{\partial R_d}{\partial H} \propto \frac{\partial X_\infty}{\partial H}; \tag{31}$$

according to Maki $\partial R_d/\partial H$ has the same angular dependence in transverse and longitudinal orientation.

In other terms for a pseudobulk sample the absorption in the domain $\theta \gg \theta_c$ and for the high-field regime is proportional to the imaginary part of the impedance of a bulk one. Since X_∞ does not decrease as sharply as R_∞, this domain is easier to explore with an electromagnet than the narrow interval $[0, \theta_c]$. Furthermore, if there is a misalignment of the sample at $\theta = 0°$, it can be neglected for large angles. The third advantage in using (22) is the expression of $\partial X_d/\partial H$ can be simplified, and under the previous conditions, one finds

$$\frac{\partial X_\infty}{\partial H}(\theta) \propto H^{-3/2}(\cos\theta)^{-1/2}(\sin\theta)^{-1} \tag{32}$$

valid as long as $e_t(\theta) \ll d$ (in our experiments this is true up to 60 deg). In (32) all the quantities can be measured by simple means in the same experiment.

For the experiments we choose PbIn samples (20-wt% In) of thickness d, $2000 < d < 3000$ Å. At 4.2 °K, the coherence length determined by the measurement of H_{c2} is $\xi \sim 210$ Å to be compared with $\delta \sim 3$ μm (estimated from the value of the dc resistivity). We work at 9.45 GHz, a frequency for which $\theta_c \sim 1°$ (the diffusion coefficient D is determined via tunnel-effect measurements of the same alloy). Results of one of our experiments are shown in Fig. 8. The slope of the transition curve is taken in the very high region. The ratio δ/ξ is larger than 10. One can see a good agreement with Maki's prediction up to 19° where a different behavior takes place. However, this type of experiment needs some comments. First of all, we have taken very few points in the first 20 deg which are the most important due to the fact that for $\theta > 30°$ it is very hard to determine $H_c(\theta)$ with precision because the main variation has taken place. This experimental imprecision restrains the comparison with Maki's calculation

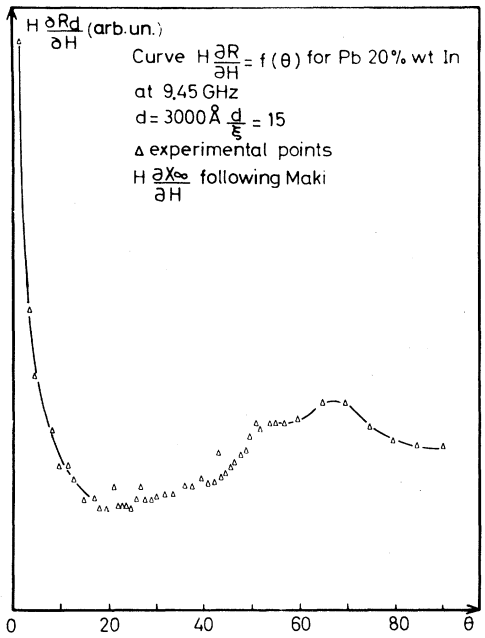

FIG. 8. Variation of the reduced slope of the superconductive transition detected by microwave absorption (9.5 GHz, longitudinal orientation) as a function of the angle θ. An agreement with Maki's prediction is obtained up to 19° but one should notice that few points have been taken in the first 20 deg.

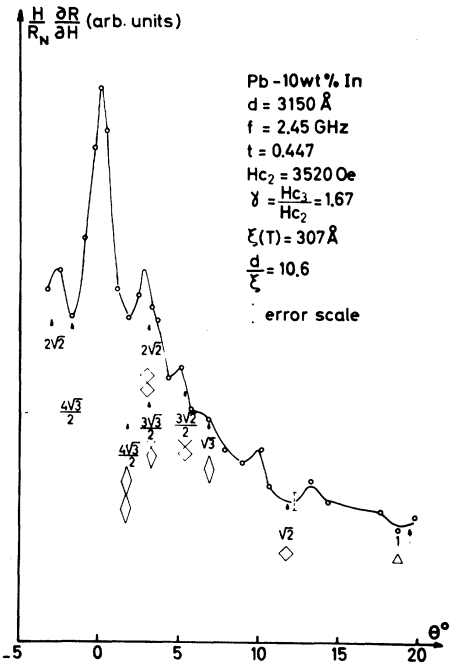

FIG. 9. Variation of the reduced slope of the normal-superconductive transition in the first 20 deg with a resolution of about 0.8° (for 2.4 GHz, transverse orientation). The variation represented in Fig. 8 is now strongly modulated. We attribute this modulation to tilted vortices. The arrows, the geometrical figures and the numbers refer to the indexation of the singularities (see Sec. III C 5).

to the first 20 or 30 deg. This is why we turn to experiments on same type of samples but with a better angular resolution. Figure 9 shows one of the typical result with a resolution of 0.8°.

The monotonic variation of $(H/R_N)(\partial R/\partial H)$ is now "modulated" by a set of extrema. In Fig. 9, the curve joining the experimental points is only drawn to give an idea of what should be the actual variation of the slope with the tilting angle. Before discussing this type of curve in more detail, we have to note that it shows that Maki's calculation cannot be fitted on a range of 20° in contradistinction to what was concluded above. However, if one considers the very first degrees of the tilting, the sharp variation of the slope predicted by Maki remains qualitatively verified.

The relatively poor precision of our experiments cannot be taken as an argument against the preceding conclusion. It is true, that from one sample to the other the curve is far from being reproducible in terms of amplitude of the slope at a given angle. But this is not too surprising if one considers the small value of the so-called characteristic angle and the fact that the surface of the evaporated sample has to be flat up to a fraction of a coherence length (about 300 Å for ξ in our experiments).

Furthermore, from one sample to the other, in spite of all the uncertainties, the extrema in the slope occur very often for the same angular value. In the same range of ideas, it is very important to remark that the curves are symmetrical under the θ to $-\theta$ transformation as it can be seen in Fig. 9.

This has suggested the study of the variation of the angular dependence when d/ξ varies. This can be realized by repeating the experiment on the same sample at two different temperatures. This avoids the chief inconvenience of comparing surface sheaths of different samples. However, the fact that θ_c varies with temperature means that we cannot expect the curve to remain invariant. One of the best results is shown in Fig. 9 and 10.

Figure 10 represents the angular dependence of the slope of the microwave-transition curve taken at the critical field on the same sample as in Fig. 9, but for $d/\xi = 8.35$ ($\xi = 390$ Å) against $d/\xi = 10.6$ and $\xi = 307$ Å for Fig. 9. The two curves, though they have the same shape, are not at all superimposable. However, the comparison of the two curves clearly shows that the extrema occur at the same angles.

In Fig. 10, there is also a dashed line represent-

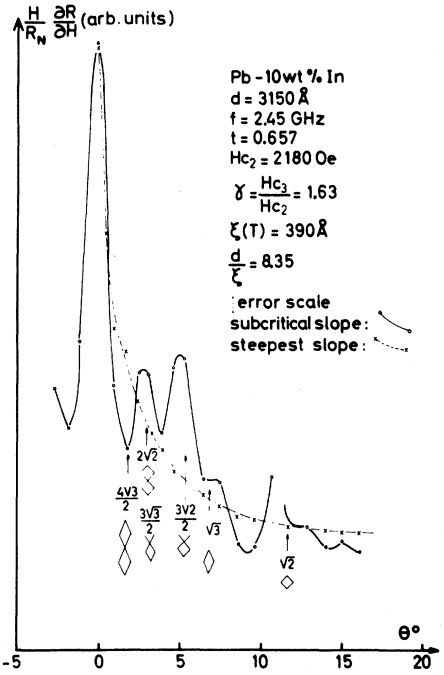

FIG. 10. Same as Fig. 9 but for a different value of d/ξ. If the variation of $(H/R_N)(\partial R/\partial H)$ is far to be equal in both cases, it is important to see that the extrema occurs for the same value of θ. The dashed line represents the normalized variation of the slope taken at the steepest part of the transition at each angle. The extremas are not observed on this variation that we call the "average variation."

ing a monotonic variation of the slope that we call "the average variation." It is, in fact, the value $(H/R_N)(\partial R/\partial H)$ not taken in the very subcritical region but in the steepest part of the transition curve. This procedure gives a second kind of determination of $(H/R_N)(\partial R/\partial H)$. We adjust it to the subcritical determination by normalizing the two determinations at $\theta = 0°$ to the same value. One can see from the dashed curve that the extrema have disappeared; this shows that the "steepest-variation" determination makes some kind of average. This is very similar to what happens for the size effect $d = 1.8\xi$ in parallel field (Sec. II). This effect is observed only if the slope is taken in the subcritical region. Thus, even if we are not able to quantitatively discuss the exact variation of $(H/R_N)(\partial R/\partial H)$ we at least have the task of explaining why the extremas of $(H/R_N)(\partial R/\partial H)$ occur for definite angles whose values are independent of d/ξ as long as $d/\xi > 1.8$, as we will see later. In other terms, the set of angular "resonances" is related to the surface conductivity and not to the thickness of the sample. The fact that they are temperature independent also means that the angular values are independent of the magnitude of the coherence length. This suggests that we have the presence of a size effect due to the presence of tilted vortices inside the surface sheath as it will be seen in Sec. III C.

C. Calculation of the geometrical structure of tilted vortices

Let us return to the detection of size effects by a surface-impedance measurement.

1. Remark on the sensitivity of microwave absorption

In Sec. II, we have seen that it is possible to detect the entrance of the first row of vortices inside a thin superconducting film when $d = 1.8\xi$. This is a size effect between the vortices and the thickness of the film. In such a situation, if we assume that the magnetic field is along the x axis and vanishes at the points

$$z = \tfrac{1}{2}d, \quad y = -\phi/k_0 + (2p+1)\pi/2k_0, \tag{33}$$

then the z axis is taken normal to the surface. ϕ is an arbitrary constant related to the arbitrary choice of the origin. k_0 is a parameter dependent on d/ξ (= 0 for $d < 1.8\xi$ and increases asymptotically towards $1.70\, d^2/4\xi^2 - d/2\xi$ when $d \to \infty$).

The microwave absorption is sensitive to the transition from an isotropic to an inhomogeneous superconductor. The inhomogeneity linked with the spatial variation of the order parameter takes place along the surface as well as normally to it.

For a normal isotropic semi-infinite metallic sample in the normal skin effect, the dissipated power P_ω inside the metal is

$$P_\omega/P_i = 4R/Z_0, \tag{34}$$

where P_i is the incident power, $Z_0 = 4\pi/c$ is the vacuum impedance, and R is the real part of the surface impedance $Z = R + iX = 4\pi\omega\sigma/c^2$. In the normal skin effect, the wave may still be taken as a plane wave near the surface inside the metal. E_ω presents an "effective" node at a distance of the order of δ from the surface, while H_ω has an antinode practically on the surface, where λ_0 is the wavelength of the microwave field in a vacuum.[16]

Let us consider now an inhomogeneous metal. This time, the skin depth is position dependent. However, as pointed out by Fisher,[17] if the sample is such that δ is everywhere much smaller than wavelength λ_0 in the vacuum, the node of E_ω is always very close to the surface, and H_ω has practically a node at $z = 0$ [the variation of H is of the order of $(\delta/\lambda_0)^2$].

P_ω is related to P_i by relation (34) using the fact that the wave is always quasiplane on the surface. The impedance in the case of an inhomogeneous metal is still defined by the usual relation

$$Z = -\frac{4\pi}{c}\frac{E_\omega}{H_\omega}\bigg|_{z=0}. \tag{35}$$

But, now, this quantity varies along the surface. Therefore, as we are not able to distinguish the contribution of each point of the surface, the experiment gives Z, but is averaged along the surface.

Returning to superconductivity, this means that in the case of a spatial modulation of the order parameter, the microwave absorption is sensitive only to its variation along the normal to the surface (as long as $d \gg \xi$, see Ref. 3).

In the case of the tilted vortices in the surface sheath, the surface impedance is also sensitive to that which occurs along the y axis, since, as soon as θ is larger than one-tenth of a degree, the distances between the intersections with the surface of neighbor vortices are much smaller than δ. On the contrary, the range of variation of the order parameter along the normal is of order ξ.

We are going to assume from now on that the "angular resonances" observed in the subcritical absorption are due to the modulation along the z axis of the surface sheath by the tilted vortices. By analogy with the case of the film of critical thickness, we assume that each time the sheath can be accommodated in its thickness and interval between two consecutive rows of tilted vortices, the absorption is affected.

Such events can occur because the surface sheath is an increasing function of θ (from 1.18ξ at $\theta = 0$ to ∞ for $\theta = \frac{1}{2}\pi$), while the number of vortices that intersect the normal to the surface is a decreasing function of θ (it vanishes at $\theta = \frac{1}{2}\pi$ since the vortices are parallel to z and increases when $\theta \to 0$).

2. *"Venetian blind" analogy*

A very naive model can help to understand the size effects induced by tilted vortices as well as their difference with the situation of first entry described in Sec. II A. Let us consider a system of blades alternatively normal and superconducting tilted with respect to the surface. In first approximation, we can suppose that the electrical field does not penetrate inside the superconducting part. The wave comes from the left-hand side of Fig. 11(a). As long as $\theta > \theta_l$, θ_l is a limiting angle defined by the situation pictured in Fig. 11(b), the wave can cross the normal blades from part to part. When $\theta > \theta_l$, a different behavior takes place; the wave is not transmitted to the right-hand side.

If b is the width of a normal blade, θ_l is given by

$$b/e_t(\theta) = \tan\theta \tag{36}$$

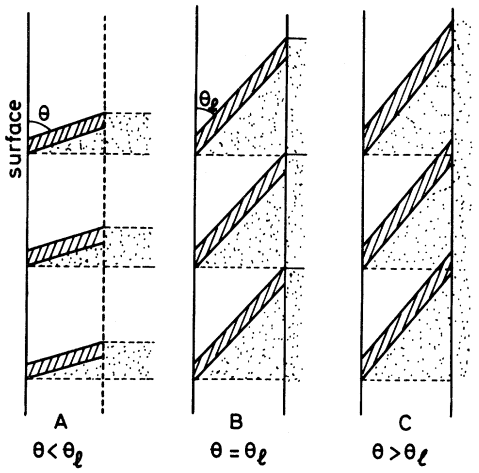

FIG. 11. "Venetian-blind" model for tilted vortices. The shaded areas or "blades" are superconducting, we assume in first approximation the electrical field does not penetrate into them. The white blades are normal. The wave comes from the left in A. Some light can cross the blind since their tilting angle is $\theta < \theta_l$. θ_l is defined by B. As soon as $\theta > \theta_l$ no more light is transmitted, this is shown by C.

(e_t being the thickness of the surface sheath). It is seen that, in spite of the fact that surface impedance is sensitive only to the variations along z, the size effect may be related to the surface "geometry" of the inhomogeneity.

This presents a striking difference with the critical-thickness case, where the condition $d = 1.8\xi$ does not take into account the periodicity of the order parameter along the surface of the thin film.

This optical model suggests also that other changes of absorption occur when one goes from a situation where any normal to the surface stands inside the same cell to a situation where it crosses many cells. This defines a set of θ_l. We call them remarkable angles.

3. *Calculation of the remarkable angles for tilted vortices*

On the surface, the origin may be chosen at will. The most convenient choice is to set it so that the plane xz, which contains the normal to the surface and the magnetic field (see Fig. 7), be a plane of symmetry. In that case, the x axis is privileged and along it there is a periodicity. We restrain our evaluation to the most simplest lattice: square or equilateral triangular.

Two possibilities are then offered: (a) the structure is a square or equilateral triangular in the plane of the surface (Kulik's assumption); (b) however, by analogy with the behavior around H_{c2}, one can think of a square or equilateral lattice in the plane perpendicular to H.

a. Square or triangular lattice in the plane of the surface. In that case, the two parameters of the vortex lattice are of the same order of magnitude and thus vary like $(\sin\theta)^{-1/2}$, while the surface sheath varies like $(\cos\theta)^{-1/2}$. Of course, we have to abandon the Venitian-blind model and turn to the exact geometrical situation. This is shown in Fig. 12 where each vortex is represented by its axis. It is seen that the remarkable angles are defined by

$$e_t = s\tan\theta . \tag{37}$$

Square lattice: using the only case considered by Kulik, one has

$$ab\sin\theta = \pi\rho_0^2 , \tag{38}$$

with

$$b = a$$

thus,

$$a^2 = \pi\rho_0^2/\sin\theta . \tag{39}$$

In the plane of the surface, two lattice orientations are possible: $a_\square$: the projection of H on the surface plane is parallel to one of the directions of the side of the elementary square; and $b_\square$: the projection of H is parallel to the direction of one of the diagonal of the elementary square. We do not consider the case where the field is parallel to other directions of translations of the vortex lattice.

In the case "$a_\square$," the singularities are associated with integer multiples of a, that is to say (Fig. 13)

$$s = na,\ n \text{ integer} . \tag{40}$$

In the case "$b_\square$," $s = na\sqrt{2}$ or $na/\sqrt{2}$. For $s = na\sqrt{2}$, the singularities correspond to vortex axis which are in the xz plane perpendicular to the film. For $s = na/\sqrt{2}$, the vortex axis responsible for the singularities are symmetrical with respect to the xz plane.

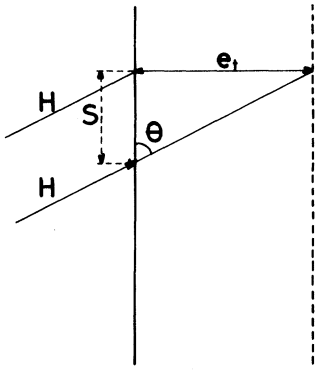

FIG. 12. Representation in the xz plane of the geometrical situation of the vortex lattice for a situation of remarkable angle. s is a multiple or an under multiple of one of the translations of the vortex lattice.

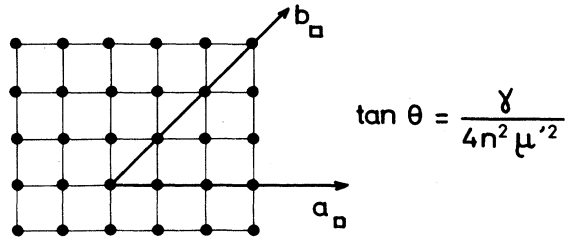

FIG. 13. Representation of the intersection of the tilted vortices with the surface in the case of a square lattice. $a_\square$ and $b_\square$ denote the directions for which the written formula is valid.

All the different situations for the square lattices are described by the equations

$$s = n\mu' a , \tag{41}$$

where

$$\mu' = 1, (1/\sqrt{2}), \sqrt{2} .$$

The condition of singularity is

$$e_t^2 = n^2\mu'^2(\pi\rho_0^2/\sin\theta)\tan^2\theta , \tag{42}$$

as $e_t^2 = \pi\rho_0^2\gamma/4\cos\theta$ [from Eq. (27)]. We obtain a very simple formula

$$\tan\theta = \frac{\gamma}{4n^2\mu'^2} . \tag{43}$$

Since μ' is given only by geometrical considerations, (43) contains no adjustable parameter.

Triangular lattice: Figure 14 shows the possible configurations: $a_\triangle$: the projection of H on the surface is along the diagonal of the elementary cell; $b_\triangle$: the projection of H on the surface is parallel to the side of the triangle;

for $a_\triangle$, $s = na\sqrt{3}/2$ or $s = na\sqrt{3}$,

for $b_\triangle$, $s = na/2$ or $s = na$.

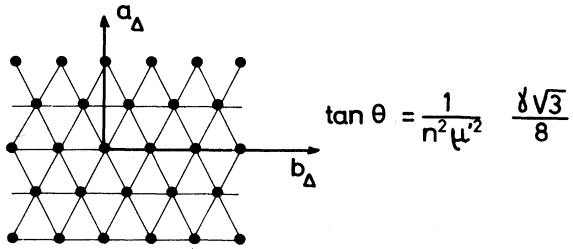

FIG. 14. Representation of the intersection of the tilted vortices with the surface of the sample in the case of a square lattice. $a_\triangle$ and $b_\triangle$ denote the directions for which the written formula is valid.

The condition of flux quantification is now

$$\tfrac{1}{2}\sqrt{3}a^2 \sin\theta = \pi\rho_0^2 \quad (\mu = \tfrac{1}{2}\sqrt{3}), \tag{44}$$

and one obtains a formula equivalent to (43), namely,

$$\tan\theta = \frac{1}{n^2\mu'^2}\,\frac{\gamma\sqrt{3}}{8}, \tag{45}$$

with $\mu' = \tfrac{1}{2}\sqrt{3}, \sqrt{3}, 1, \tfrac{1}{2}$.

b. Square or triangular lattice in the plane perpendicular to the magnetic field. In this case, the condition of quantization is

$$\mu\alpha\beta = \pi\rho_0^2, \tag{46}$$

where α and β are elementary translations in the plane perpendicular to H. We can again develop the same discussion on the relative position of the lattice in the plane xz.

The basic configuration in this plane is represented in Fig. 15. The quantity s is now replaced by s'. The condition of remarkable angle is now

$$s' = e_t \cos\theta \tag{47}$$

and we also have

$$s' = n\alpha, \quad n \text{ integer}. \tag{48}$$

Note that $\mu' = 1$ since we are in a plane perpendicular to H.

Using expression (19) for e_t yields

$$\cos\theta = 4n^2/\mu\gamma. \tag{49}$$

Even for $n = 1$ and $\mu = \tfrac{1}{2}\sqrt{3}$ (maximum value) $4n^2/\mu\gamma > 1$ so that no real value of θ may be obtained whatever n and μ. This means that, if the lattice is square or triangular in a plane perpendicular to H, there is no remarkable angle. Therefore, according to our hypothesis of interferences between the tilted vortices and the surface sheath, the vortex lattice cannot be square or triangular in a plane perpendicular to H. Though his choice of a square lattice along the surface was not justified by Kulik,[10] our simple geometrical considerations support the idea that the vortex lattice should be square or equilateral along the surface.

4. Validity of the geometrical model

The above remark may be retained as an argument in favor of our model. A second argument lies in the fact that Eqs. (43) and (45) are independent of ξ, in agreement with the experimental observations. Note, however, that any model which relies on a "size effect" between tilted vortices and the surface sheath, would bring, for the remarkable angles, expressions independent of ξ.

A third argument is that, numerically, (43) and (45) may account for the experimental results. Indeed, as is shown in Sec. III C 5, the singularities

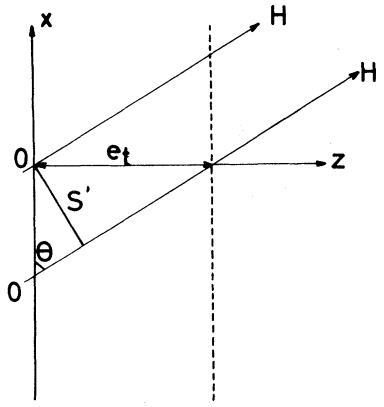

FIG. 15. Representation in the plane xz of a situation of remarkable angle in the case where it is assumed that the vortex lattice is triangular in the plane perpendicular to the magnetic field.

of the absorption curves may be indexed without any ambiguities. It must be kept in mind that our model is only *putative*. Indeed, we have restricted our discussion to geometrical considerations based on the plausible assumption that the singularities are due to the accommodation of vortex rows in the surface sheath. We have not computed the repartition of vortices in the slab, and *a fortiori* the corresponding time-dependent absorption. As mentioned above, the determination of the vortices configuration implies an involved process of energy minimization and the solution of the Ginzburg-Landau equation (5) in the presence of the cross term.

5. Indexing of the remarkable angles

We shall now return to our geometrical assumption. If the repartition of the vortices had been computed from the Ginzburg-Landau equation, for each value of H and θ, the nature of the lattice would have been determined. Therefore, for each critical value θ_{cr} of the angle, one would have known which "theoretical" formula (43) or (45) holds. In the absence of such a calculation the situation is reversed; we obtain from experiment the values of θ_{cr} and we check whether (43) or (45) holds and deduce the nature of the lattice for each particular angle.

The result of this indexing process is reported in Figs. 9 and 10. The agreement is remarkable for five singularities (better than 0.3° for an angular resolution of 0.8°), between 0° and 15°. However, two singularities at 4.2° and 10° cannot be accounted by (43) or (45).

Despite of these two exceptions, the results are surprisingly good, considering (i) the poor precision of the determination of $(H/R_N)(\partial R/\partial H)$;

and (ii) the fact that (43) and (45) do not contain any adjustable parameter. We consider this remarkable agreement a further argument in favor of our model. We have no satisfactory explanation for the singularities at 4.2° and 10°.

In Figs. 9 and 10, we have represented the geometrical situation for each indexed singularity. The numerical values refer to the quantity $n\mu'$. The geometry of the vortex rows which are accommodated is represented for each case. In these representations, the projection of the magnetic field on the surface is always the vertical axis.

It appears that for most of the singularities, the projection of H is always along the diagonal. The smaller the value of θ, the higher the number of rows. We detect up to four rows in the surfaces. According to this model, the vortex structure seems to be alternatively triangular or square. The first row of vortices in the surface sheath appears for 20.1° in the triangular structure ($\mu' = 1$) and 22.9° ($\mu' = 1$) in the square structure. Only for this value of μ', the projection of the fields is parallel to the side of the cell and we are not able to distinguish between these two predicted singularities. However, it is at this value of θ that the "averaged" curve $(H/R_N)(\partial R/\partial H)$ (the one obtained with an angular resolution of 2° or 3°) no more follows a Maki-type variation.[18]

In conclusion, we might say that the indexing works quite well and is an argument in favor of our putative model. The reader may be somewhat amazed that the vortex lattice in the sheath may change alternatively from triangular to square. An argument in favor of this possible alternative may be found in a work by Lasher[19] who computed the behavior of a small type-I specimen ($d \ll \xi$) and found that the system may easily go from triangular to honeycomb lattices with several quanta of flux per cell. Indeed the free energies of the triangular and square lattices are very close to each other (in the perpendicular situation) and it is possible that, in the case of a sheath somewhat similar to a thin film, the free energies of the two type of lattices may be alternatively bigger and smaller.

IV. TILTED VORTICES IN NONHOMOGENEOUS SUPERCONDUCTORS

By nonhomogeneous superconductors, we mean hereafter superconductors having a spatial modulation of the order parameter. This is the case for (i) thin films where d is of the order of some coherence length, and (ii) multilayered compounds.

A. Tilted vortices in thin films

A priori, it is suggested to try an extension of our model to films whose thickness is of the order of a few coherence lengths. Such samples are no more bulk samples and one may think that, in a tilted field, there is an interaction between the two surface sheaths. In fact, this interaction is dominant and, if one considers $(H/R_N)(\partial R/\partial H)$, one gets a great number of singularities and we are no more able to apply our model even at small angles as soon as $d \lesssim 5\xi$. The situation can only be described qualitatively; the notion of two distinct surface sheaths is no more valid. A de Gennes–Saint-James vortex structure is present in the middle of the film and has an interaction with the tilted vortices. As long as the angular resolution of the experiments is not greatly improved, there is no hope for a phenomenological description of the vortex structure.

B. Multilayered compounds

In this case, the spatial modulation of the order parameter is due to the fact that the bulk sample is constituted by a stack of alternatively normal and superconducting slabs. Thus, far from the GL region, the superconductivity spreads all over the sample and in a tilted field, we can have pinning of the hard-core vortex by the normal slabs. The discussion is analogous to that concerning our previous model because this time the z axis normal to the surface is also the c axis of the crystalline structure. As the problem is invariant in a translation parallel to a slab, we have to discuss the equation of the singularities along the c axis (Fig. 16).

The two equations of the problem are the condition of singularity (pinning)

$$nd^* = l, \tag{50}$$

where l is the distance between two vortices mea-

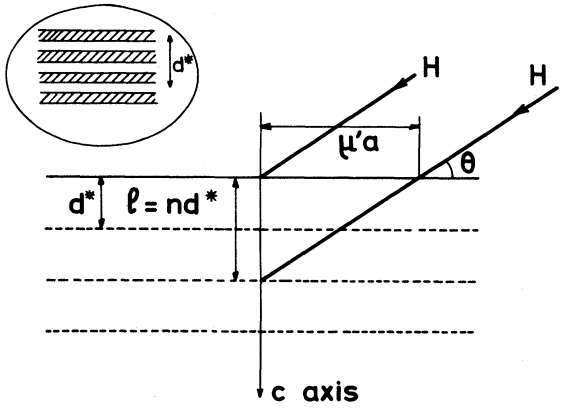

FIG. 16. Geometrical situation of tilted vortices in a multilayered superconducting compounds. The insert represents the actual situation for TaS_2 +pyridine at 32 kG and 2.81°K.

sured along the c axis, d^* is a characteristic length of the crystal. d^* is not necessarily equal to d, the actual crystalline period, because the section of the vortex might be of the same order of magnitude as d. We expect d^* to be equal to pd (p integer); it has the meaning of the crystalline period as "seen" by the vortex array.

We have also the flux quantification condition expressed by Eq. (16) where, we have

$$l = \mu' a \tan\theta , \tag{51}$$

and finally,

$$\frac{\sin\theta}{\cos^2\theta} = n^2 d^{*2} \frac{\mu}{\mu'^2} \frac{H}{\phi_0} . \tag{52}$$

This geometrical formula introduces no adjustable parameter but d^*.

Let us apply (52) to the case of the recently published dc resistive measurements on TaS_2 + pyridine.[21] The authors study the angular dependence of the resistivity in tilted field. An unexplained series of oscillations is found (Fig. 17).

The multilayered compound TaS_2 + pyridine has the same thickness for the slabs of TaS_2 as for the slab of pyridine, 6 Å. Thus, this length is d in spite of the fact that the actual crystalline period is 12 Å.[22] Due to that coincidence, the model calculates pinning as well as antiminimum pinning situations. In a recent paper,[20] a new phase with d = 11.85 Å is studied. This means an uncertainty of 3% in d^{*2} which does not affect significantly the quality of the results. The size of one vortex is in the range 10–20 Å (it is an ellipsoidal vortex); thus d^* can be chosen in the 20–40-Å range (let us recall that in a bulk type-II at H_{c2} the spacing between vortices is 2.7 times the coherence length). This left three values of d: 24, 30, 36 Å.

We present in Table I all the possible values for d^* = 30 Å. The experimental θ's are also given and the underlined values correspond to the choice of indexing. Within the angular precision, we have five indexed singularities. Since Eq. (52) has a d^{*2} dependence, this justifies the choice of d^*.

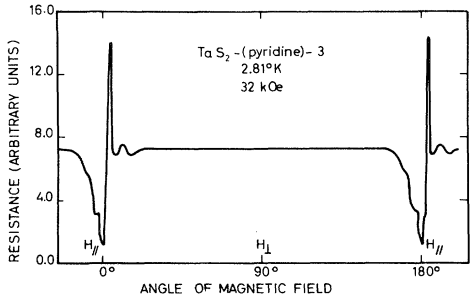

FIG. 17. Angular dependence of the resistance of a sample of TaS_2 +pyridine as published in (19). The plateau after 25° corresponds to the normal state. We interpret the oscillations before as the pinning or antipinning of tilted vortices by TaS_2 on pyridine slabs.

In contrast with the situation of an homogeneous bulk type-II superconductor, we see that the model suggests (more experiments are needed) that the lattice is square along the surface at small angles but become triangular for higher values. But again, it is only putative because we made no evaluation of the energy. However, we think that it shows that multilayered components are a good candidate for periodic pinning.[23]

V. CONCLUSION

A detailed study of subcritical behavior of type-II superconducting films of various thickness shows that microwave absorption provides information on size effects in parallel field at the subcritical thickness ($d = 1.8\xi$). In tilted field, microwave absorption exhibits a behavior quite different from a theoretical prediction. Numerous singularities are present where angular values are independent of d/ξ, as long as this ratio is large. We interpret these singularities as the interference of tilted vortices lattice with the surface sheath.

A geometrical putative model is proposed that is in good numerical agreement with the best experimental data. This model can be, with minor modification, extended to multilayer superconducting compounds.

ACKNOWLEDGMENTS

We thank M. Boix and Y. Brunet for their participation in the experimental work.

APPENDIX A: MICROWAVE BENCHES AND SAMPLE PREPARATIONS

We use two benches for microwave absorption working, respectively, around 2.35 and 9.45 GHz. Both are based on the principle of a four-post device. The generator is in one post; the opposite post contains the resonant cavity where the film is sticken of the wall; the third post is used to compensate the reflected power from the cavity and the crystal detection is on the fourth post. The klystron generator is frequency stabilized on the cavity via a lock-in detector. The Q of the resonant system is about 800 for the unloaded cavity. By measuring the ESR linewidth of a monovalent copper salt, we got an evaluation of the sensitivity of the system: 10^{14} spins/G (we have no field modulation). The cavity is a parallelipedic rectangular box at 9.45 GHz, a U-shape resonator at 2.35 GHz. Each is isolated from the helium bath by a thermostated box in which there is a residual pression of helium. The tempera-

TABLE I. $\theta°$ calculated from the model for $d^*=30$ Å and experimental θ's.

Vortex intersection with a layer of thickness d^*	Square	Square diagonal	Equilateral	Equilateral diagonal
$n=1$	0.83	1.66	0.72	0.96
$n=2$	3.33	6.59	2.88	3.84
$n=3$	7.49	14.22	6.49	8.50
$n=4$	12.98	23.13	11.20	14.56
$n=5$	18.5	31.75	16.70	21.35
Experimental θ's	1.13 ± 0.4 3.44	6.60	11	14.83

tures are measured by a carbon resistor glued near the sample and they are stabilized by a heating device supplied through an amplifier by the signal constituted of the difference between the fixed and the actual value of the resistor thermometer 10^{-3} °K stability is achieved. By measuring the critical field H_{c3} at the beginning and the end of the recording of curves $R(H)$ at T, θ fixed, we are not able to see a variation of its value. Due to the field configuration of each resonator, the recordings at 10 GHz are made in a longitudinal orientation, whereas we are in the transverse orientation with the 2.45-GHz cavity.

Preparation of the samples

The metallic films are obtained by evaporation under vacuum (10^{-6} Torr) of a small quantity of the *Pb*In alloy from a crucible heated by Joule effect. The substrate of the film is a quartz slab $0.2\times7\times7$ mm optically polished and then heated by a flame. During the evaporation, this substrate is kept at 200 °K (with liquid-nitrogen cooling) or at room temperature. The cooling is useful for the realization of continuous thin films ($d\leq800$ Å).

Each substrate is covered on its borders by "Magic tape" in order to leave free for the deposition a 5×5 mm^2. The "Magic tape" is removed after evaporation and thus the film has straight edges. This is not very useful for our experiments since microwave absorption is proportional to the area irradiated but it helps to measure the thickness optically. A Normarsky interferometer is used and a precision of ±100 Å is achieved for films of thickness over 800 Å.

The optical determination of the thickness is compared with the value deduced from critical film measurements by the formula

$$d^2 = (6\phi_0/\pi)H_\perp/H_\parallel^2 . \tag{53}$$

The agreement between the determination is a criterium of the film quality.

The crucible is at 250 mm of the substrate in the evaporator. This authorizes a realization of several films in the same process. When they are side by side, we have verified that they exhibit no differences in their superconducting properties. Therefore, at the scale of one sample, we are sure that the gradients of concentration are negligible.

APPENDIX B: SURFACE IMPEDANCE OF PSEUDOBULK SAMPLES ($\xi \ll d \ll \delta$)

Maxwell's equations are

$$\mathrm{div}\vec{D} = 0 , \tag{54}$$

$$\mathrm{div}\vec{B} = 0 , \tag{55}$$

$$\mathrm{rot}\vec{H} = \frac{4\pi}{c}\vec{J} + \frac{1}{c}\frac{\partial\vec{D}}{\partial t} , \tag{56}$$

$$\mathrm{rot}\vec{E} = -\frac{1}{c}\frac{\partial\vec{B}}{\partial t} . \tag{57}$$

As it is explained in Sec. III C 1, we are in the plane-wave approximation even when tilted vortices are present. Thus, the microwave magnetic field can be considered as the superposition of an incident and a reflected wave

$$H = Ae^{-kz} + Be^{+kz}, \quad k = (1-i)/\sqrt{2}\delta . \tag{58}$$

The interface conditions are (see Fig. 18)

$$A + B = H_\omega(0) \quad \text{in } z = 0 , \tag{59}$$

$$Ae^{-kd} + B^{ekd} = pH_\omega(0) \quad \text{in } z = d , \tag{60}$$

with $|p|<1$. The surface impedance is, in general,

$$Z_d = \frac{c}{\sigma H_\omega(0)}\left.\frac{dH_\omega}{dz}\right|_{z=0} = \frac{ck}{\sigma}\frac{e^{kd}+e^{-kd}-2p}{e^{-kd}-e^{kd}} \tag{61}$$

(we applied the relation $J=\sigma E$). For a bulk sample $d=\infty$, thus

$$Z_\infty = -ck/\sigma . \tag{62}$$

For $|kd|<1$, we have at the first order in

$$Z_d = Z_\infty(1-p)/kd . \tag{63}$$

From (59) and (60) and the equation of continuity

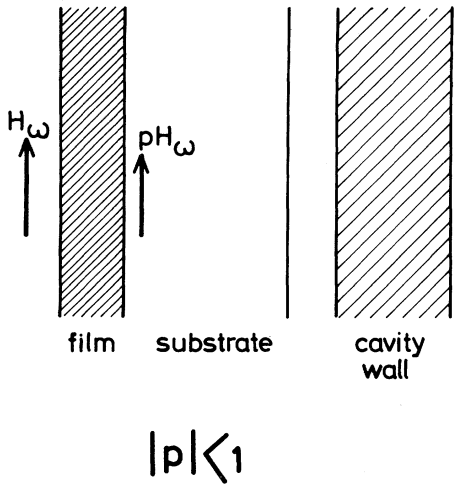

FIG. 18. Schematic representation of the microwave magnetic field when a thin film ($d \ll \delta$) is sticken on the wall of the cavity (see Appendix B).

at the interface film cavity (we neglect the effect of the quartz substrate because we are far from optical wavelength),

$$(k/\sigma)(-Ae^{-kd} + Be^{kd}) = -(k_c/\sigma_c)pH_\omega(0) \tag{64}$$

(the index c is for the wall of the cavity), we got

$$p = \frac{(k/\sigma)(1+\coth kd)e^{-kd}}{(k/\sigma)\coth kd + k_c/\sigma_c}. \tag{65}$$

Since we have "dirty" alloys, the conductivity in the wall of the cavity is higher than in the film

$$\frac{k_c}{\sigma_c} \sim \frac{1}{\sqrt{\sigma_c}} \ll \frac{1}{\sqrt{\sigma_N}} \sim \frac{k_N}{\sigma_N}, \tag{66}$$

where N denotes the normal state of the film

$$p_N \sim (1 + thk_N d)e^{-k_N d}. \tag{67}$$

For $k_N d \ll 1$, we got

$$p_N = 1 - \tfrac{1}{2}k_N^2 d^2, \tag{68}$$

$$Z_d^N = \tfrac{1}{2}k_N d Z_\infty^N. \tag{69}$$

In the superconducting state, the conductivity of the film becomes σ_1 and (66) is not necessarily verified. However, in the subcritical region $\sigma_s \sim \sigma_N$ and we can again neglect k_c/σ_c before k_s/σ_s and p_s are given by (67), where k_N is replaced by k_s.

For a thick sample $\xi \ll d$ in the surface sheath regime, we cannot keep $k_s \sim k_N$ and p as given by (68). Roughly, we can consider the sample as superconducting is a slab of thickness ξ and normal in the middle of the sample. The correction $\Delta k = k_s - k_N$ is proportional to ξ/d; we have at the first order

$$\Delta k \sim (\xi/d) f(\sigma_s - \sigma_N). \tag{70}$$

On the contrary, Z_∞ remains a local quantity in the sense that only the surface properties are involved in its modification:

$$\Delta Z_\infty \sim g(\sigma_s - \sigma_N), \tag{71}$$

where $g(\sigma_s - \sigma_N)$ is a function of the same order of magnitude as f; but the superconducting region is only a small part of the sample so we can neglect the correction to k and therefore to p, before the correction to Z_∞ (this means implicitly that we stay in the subcritical region)

$$\frac{1-ps}{k_s d} \neq \frac{p_s d}{2} \neq \frac{k_N d}{2} = \frac{1-i}{2\sqrt{2}}\frac{d}{\delta}, \tag{72}$$

$$Z_d = \frac{1}{2\sqrt{2}}\frac{d}{\delta}[(R_\infty + X_\infty) + i(R_\infty - X_\infty)]. \tag{73}$$

The expression is valid in the normal and the superconducting state with the above restrictions.

In the normal state, $R_\infty = X_\infty$, Z_d is purely real and

$$\mathrm{Re}(Z_d) = \frac{1}{2\sqrt{2}}\frac{d}{\delta}(R_\infty + X_\infty). \tag{74}$$

Equation (74) is applied in the experimental discussion of Maki's theory for angular dependence of microwave absorption (Sec. III B).

[1]E. Guyon, F. Meunier, R. S. Thompson, Phys. Rev. 156, 452 (1967).
[2]R. S. Thompson, Phys. Rev. B 1, 327 (1970).
[3]Y. Brunet, E. Guyon, W. Holzer, P. Monceau, and G. Waysand, in *Proceedings of the Thirteenth International Conference on Low Temperature Physics, Boulder, Colo., 1972,* edited by R. H. Kropschot and K. D. Timmerhaus (University of Colorado Press, Boulder, Colo., 1973), Vol. 3, p. 156.
[4]W. Holzer, G. Waysand, and E. Guyon, in *Proceedings of the Twelfth International Conference on Low Temperature Physics,* edited by Eizo Kanda (Keigaco, Tokyo, 1970), p. 497; and G. Waysand, thesis (Orsay, 1972) (unpublished).
[5]J. Sutton, Proc. Phys. Soc. Lond. 87, 791 (1966).
[6]A. A. Abrikosov, Zh. Eksp. Teor. Fiz. 32, 1442 (1957) [Sov. Phys.—JETP 5, 1174 (1957)].
[7]M. Tinkham, Phys. Lett. 9, 217 (1964).
[8]D. Saint-James, Phys. Lett. 16, 218 (1965).
[9]K. Yamafugi, E. Kusayanagi, and F. Irié, Phys. Lett. 21, 11 (1966).
[10]I. O. Kulik, Zh. Eksp. Teor. Fiz. 55, 889 (1968) [Sov.

Phys.-JETP 28, 461 (1969)].
[11]P. Monceau, thesis (Grenoble, 1970) (unpublished).
[12]C. Caroli and K. Maki, Phys. Rev. 159, 306 (1967).
[13]K. Maki and G. Fischer, Phys. Rev. 184, 472 (1969); and Y. Brunet, P. Monceau, and G. Waysand, Phys. Rev. B 10, 1927 (1974).
[14]K. Maki, J. Low Temp. Phys. 3, 545 (1970).
[15]K. Maki, *Tokyo Summer Lectures on "Physics of Quantum Fluids"* (Syokabo, Tokyo, 1971), p. 117.
[16]See, for example, J. D. Jackson, *Classical Electrodynamics* (Wiley, New York, 1962), p. 239.
[17]G. Fischer, L'impédance de surface de métaux dans les états supraconducteurs et normaux. Symposium de Physique des Solides, Saint-Hilaire, Quebec (1970) (unpublished).
[18]P. Monceau, D. Saint-James, and G. Waysand, in Ref. 3, Vol. 3, p. 152.
[19]G. Lasher, Phys. Rev. 154, 345 (1967).
[20]A. H. Thompson, Solid State Commun. 13, 1911 (1973).
[21]R. C. Morris and R. V. Coleman, Phys. Rev. B 7, 991 (1973).
[22]F. R. Gamble, F. J. Di Salvo, R. A. Klemm, and T. H. Geballe, Science 168, 568 (1970).
[23]S. H. Autler, J. Low Temp. Phys. 9, 241 (1972).